

Received March 11, 2019, accepted March 25, 2019, date of publication April 15, 2019, date of current version May 21, 2019.

Digital Object Identifier 10.1109/ACCESS.2019.2910352

Distributed Reactive Power Control and SOC Sharing Method for Battery Energy Storage System in Microgrids

WENFA KANG¹, (Student Member, IEEE), MINYOU CHEN¹, (Senior Member, IEEE),
BO LI¹, (Student Member, IEEE), FEIXIONG CHEN², (Member, IEEE),
WEI LAI¹, (Member, IEEE), HOUFEI LIN³, AND BO ZHAO⁴

¹The State Key Laboratory of Power Transmission Equipment & System Security and New Technology, School of Electrical Engineering, Chongqing University, Chongqing 400044, China

²School of Electrical Engineering and Automation, Fuzhou University, Fuzhou 350108, China

³State Grid Zhejiang Pingyang Power Supply Company, Hangzhou 325400, China

⁴Electric Power Research Institute, State Grid Zhejiang Electric Power Company, Hangzhou 310014, China

Corresponding authors: Wei Lai (laiweicqu@126.com and Minyou Chen (mchencqu@126.com))

This work was supported in part by the Science and Technology Project of State Grid Zhejiang Electric Power Company under Grant 5211W4180001, and in part by the National 111 Project of China under Grant B08036.

ABSTRACT Battery energy storage system (BESS) is a pivotal component to increase the penetration of renewable generation and to strengthen the stability and reliability of the power system. In this paper, for the purpose of the state of charge (SOC) balancing and reactive power sharing, a multiagent system (MAS)-based distributed control model, which contains a top layer communication network built by agents and a bottom-layer microgrid composed of BESSs, distributed generators (DGs), and Loads, is provided. Next, a systematic method is designed to build the control laws for agents from any given network, where each agent on the top communication network collects the states of BESSs, DGs it connects and exchanges information with its neighboring agents. Moreover, two theorems, which provide guidelines to design distributed control laws for SOC balancing and reactive power sharing between BESSs, are proposed to show the convergent property of the proposed control laws. Furthermore, several simulation cases are employed to validate the effectiveness of the proposed control model when environmental conditions and time-varying load demands are considered. Finally, the simulation results verify the effectiveness of the proposed control model, i.e., the SOC balancing and proportional reactive power sharing are achieved as expected. Furthermore, our approach has the fast convergent speed of SOC balancing of BESSs, compared to the existed method.

INDEX TERMS Battery energy storage system (BESS), distributed control, state of charge (SOC) balancing, reactive power sharing, microgrids.

I. INTRODUCTION

With the increasing of worldwide market demand, the proportion of renewable energy sources to conventional energy sources is going higher in recent decades. Further, renewable energy is strongly considered to be a solution of environmental pollution and a promising substitution of the burning of fossil fuels for power generation [1]. However, the intermittence of renewable power resources, such as photovoltaic generation systems (PVs) and wind turbines (WTs), usually brings negative impacts to the grid. To address

these problems, the integration of battery energy storage systems and renewable DGs into an MG draws extensive attention. An MG, which contains DGs, loads, energy storage systems and other devices, is an effective integration of renewable DGs into the main grid when it works in a grid-connected mode [2]. Moreover, energy storage systems, such as battery energy storage systems (BESSs) and electric vehicles (EVs), play an important role to balance system load demand, smooth the intermittence of renewable DGs, achieve peak-shaving and valley-filling purposes [3]–[5], etc.

Inevitably, an MG that contains BESSs, renewable DGs and loads can operate in a grid-connected mode aimed at enhancing the penetration of renewable DGs. A most

The associate editor coordinating the review of this manuscript and approving it for publication was Liang Hu.

straightforward approach, termed centralized control, has been widely adopted in the control of MG to manage energy storage systems [6]–[13] where the main effort is spent on designing strategy to keep SOC of the BESSs balanced for the reason of preventing overcharging or over-discharging as well as maximizing the power capacity of the overall BESSs. In [7], centralized control strategies for SOC balancing in microgrids are proposed for battery energy storage systems, while centralized optimal power flow strategies are designed in [8], [9] to optimize power flow between the main grid and the microgrid. However, the centralized control approach needs the MG central controller (MGCC) to communicate with all loads, DGs and BESSs, and then the MGCC sends the control decisions back to DGs and BESSs. Therefore, a fast and reliable communication network and powerful central controller are required due to processing significant amounts of data. Moreover, the single-point failure is a disadvantage of centralized control, since any failure of the MGCC or its associated communication links will affect the entire system [14].

Nowadays, distributed control methods [15]–[22] draw intense attention among researchers. Distributed approaches have the ability to avoid the single-point failure, high communication system costs as well as high computation load. Therefore, applications of distributed methods including microgrids control [15], energy management [23], economical power dispatch [15], SOC balancing [22], reactive power sharing [24] and frequency control [25] are various. However, several challenges of designing distributed control methods are non-negligible. To begin with, dealing with intermittent generation and time-varying demand in a distributed way isn't a trifle problem in islanded microgrids [16]. Secondly, designing the feedback control gain, which is often related to system performance, for distributed control laws is vital to system stability [26]. Last but not least, distributed control methods are susceptible to communication constraints, such as, communication delays and packet losses, therefore, designing the distributed robust control methods is demanding [25], [27], [28].

In spite of challenges, distributed control methods is a potential way to increase system reliability and scalability [17]–[19]. For example, in [17], a nonlinear distributed controller for power sharing was proposed when the consideration of dynamical models of PVs, battery energy storage systems and plug-in hybrid vehicles are incorporated. Additionally, decentralized communication-less control methods for power management of a PV/battery unit were provided to maintain system power balanced and frequency stable while considering the limits of SOC of the battery [18], where the outputs of PV are reduced to protect the overcharge of battery when frequency is high, on the contrary, the noncritical loads are regulated to prevent battery from over-discharge. While in [19], decentralized power management strategy based on multi-segment P/f characteristics, which takes load demand, renewable generation and SOC of batteries into consideration, was proposed to handle multiple PV/battery systems in islanded microgrids.

Focusing on the SOC balancing problem between BESSs, Morstyn *et al.* designed a distributed approach for reconfigurable batteries by adopting dynamic consensus algorithm [20]. By employing consensus-based leader-follower strategy, Golsorkhi *et al.* [21] utilizes a V-I droop mechanism to balance the SOC and manage the power of BESSs. Moreover, to achieve the SOC balancing, Cai *et al.* designed a set of distributed control laws for grid-connected BESSs, where two consensus algorithms are utilized to estimate the SOC and average output power of BESS [22]. Xu *et al.* proposed a two-layer distributed robust control model for grid-connected inverters to keep the SOC balancing of BESS, where the proposed distributed SOC balancing algorithms need to transmit the information of the local power supply-demand mismatch and BESS SOC balancing state variable. After communicating with the neighboring agents, then the set-points of BESSs are calculated and sent to their lower control devices. However, during the iteration, the SOC of battery is assumed to be unchanged [29]. In [30], a non-linear consensus law was proposed for grid-connected MG, where some complicated requirements need to be satisfied. Discrete consensus algorithm, which was adopted in [31], plays a role of sharing the information of SOC of BESSs and adjusting the d-axis virtual resistor to produce the active power according to the values of SOC. Continuous consensus control is adopted in [32] to adjust the outputs of batteries to achieve SOC balancing, in which the penetration of renewable energy sources isn't considered and the secondary frequency control model is needed to generate the set-points for batteries.

Moreover, multiagent system (MAS) has been widely introduced to distributed control, optimization and energy management for MGs [23], [33]–[35]. For example, an MAS based frequency control method was studied for MGs, where agents only share information with its neighbors according to consensus algorithm [25]. Further, by adopting MAS, Bidram *et al.* [26] proposed a distributed secondary control mode for MGs. In addition, MAS-based control strategies for SOC balancing among battery energy storage system have also been introduced for MGs. Based on droop control, reference [36] proposed a distributed strategy to regulate BESSs to balance the system energy, as well as the stability of system frequency. In [37], the global average values of SOC were found by a dynamic average consensus algorithm, and it was added into droop control model to regulate the active power of BESSs to achieve SOC balancing. Moreover, distributed hierarchical control method for BESS was proposed in [28], where active/reactive power sharing and energy sharing were achieved by implementing the designed fast consensus algorithm into droop controller.

In summary, most of the proposed SOC balancing methods mentioned above, such as methods in [18], [19], [21], [28], [32], [36], [37], where first-order consensus algorithm was the main route to share the information of SOC and system power among BESSs, were carried out on the droop-based platform. As we know, in grid-connected MGs, the

droop-control-based approach may not be applicable due to the fact that the system voltage and frequency are both dominated by the main grid. However, a few references, for instance, approaches mentioned in [22], [29], [30] are focusing on discussing the distributed SOC balancing for grid-connected BESSs, where the drastic fluctuation of renewable generation and load demand aren't well considered. Moreover, the distributed methods proposed in these papers need to satisfy some complicate requirements in order to accomplish the balancing of SOC. In order to provide a simple but efficient strategy for SOC balancing and reactive power sharing of BESSs, a distributed agent-based control framework, which contains two layers (communication layer and MG layer), is proposed in this paper. For communication layer, the distributed second-order algorithm, which has fast convergent speed of SOC, is first introduced to achieve SOC balancing of BESSs. Compared with methods in [22], only one kind of second-order algorithm is needed in our method, which reduces complexity to design control laws for SOC balancing. Later, aiming at guaranteeing the proportional dispatch of reactive power among BESSs, the simplified distributed control laws are provided. Further, the proposed SOC balance control laws and the reactive power sharing control laws can guarantee the system active and reactive power balanced during the iteration, respectively.

Inspired by the distributed control approaches for MGs, we extended our previous works [27], [38] into the present one. As is shown in [38], the agent-based distributed control model for islanded MGs was designed to achieve the optimal active power dispatch considering drastic fluctuation of renewable energy sources and loads. Later, in [27], we simplified the agent-based communication network and therefore proposed a fully distributed control strategy for islanded MGs, where communication loss was also considered. Based on these efforts, we proposed a distributed control strategy, which only needs the local information of the active outputs of BESS, the value of SOC and reactive power, to guarantee the SOC balancing of BESSs and proportional reactive power sharing. As noted above, two main differences are:

- 1) We designed a distributed strategy for MGs where only controllable agents and the PCC agent are utilized to compose the communication network which simplifies the designing of distributed control laws and reduces the investment of communication system, compared with the work [38].

- 2) Compared with the work [27], improvements are introduced. Such as, the second-order distributed control laws are offered to adjust the outputs of BESS while achieving the balance of SOC and system power simultaneously. Moreover, the proposed distributed control laws for optimal reactive power dispatch are simplified.

In this paper, a distributed MAS-based control method for the SOC balancing and reactive power sharing in grid-connected MGs is proposed. The control approach consists of two layer, in which the bottom layer is an

MG composed of load, BESSs and renewable DGs, while the top layer is a communication network formed by agents for secondary control. And the main contribution of the proposed control approach is:

- (a) a fully distributed control model for the SOC balancing and reactive power sharing in MGs is presented, each agent only needs local information, i.e., the values of active power, SOC and reactive power of its neighboring agents, to finish the given task;

- (b) the SOC balancing of BESSs is achieved by the proposed second-order control laws, where the strong assumption that SOC of BESSs is a constant during iteration [29] is unnecessary. And, compared with the methods in [30], some complicate requirements for distributed control laws are undesired;

- (c) compared with the method in [32], the proposed method is lack of extra computation of Riccati equation to calculate the control gains, which leads to high scalability. Moreover, the proposed control laws have faster convergent speed of SOC;

- (d) the power balance and convergence property of two sets of control laws are proved by the proposed theorems which give guidelines for designing the distributed control laws for agents from any given network.

The rest of this paper is organized as follows. The two-layer distributed control model for the SOC balancing and reactive power sharing is formulated and presented in Section II. In Section III, the power balance and convergence property of control laws are analyzed by the proposed theorems. Thereafter, the structure and parameters of the grid-connected MG are introduced in Section IV. Later, five simulation cases are designed to evaluate the effectiveness of proposed method and simulation results are analyzed and discussed. Section VI concludes the paper.

II. CONTROL METHOD FOR MGS

In this section, some terms that are used in the paper are introduced first. Next, the proposed distributed control model for MGs is designed, where the topology of communication network composed of agents is explained in detail. Thereafter, the distributed SOC balancing control laws and the distributed reactive power sharing control laws for BESS are presented in subsection *B* and *C* respectively.

A. THE TOPOLOGY OF COMMUNICATION NETWORK

As shown in Fig.1, the proposed model is built up by two layers, where the top layer is a communication network composed of agents, while the bottom layer is a microgrid which contains DGs, BESSs and loads. In microgrids, photovoltaic systems (PVs) or wind turbines (WTs) are regarded as *uncontrollable* DGs, as the outputs of these DGs are largely influenced by environmental conditions. Besides, the battery energy storage systems (BESSs), are regarded as *controllable* DGs, since their outputs can be regulated.

In comparison with the MG in which power flows, there is a directed communication network $G(V, E)$ over the MG,

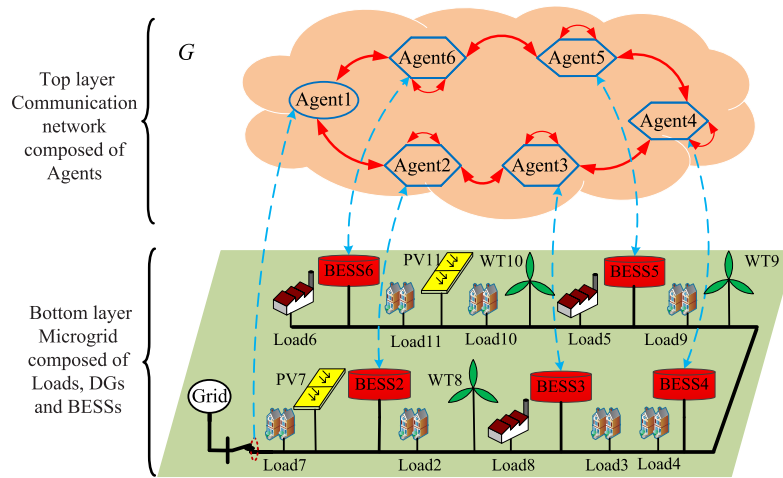


FIGURE 1. The two-layer control model for an MG, where uncontrollable agents are indicated by circles, while controllable agents are indicated by diamonds. Besides, the dash lines between the two layers indicate the relationships among agents and their connecting DGs, BESSs and loads, and the arrows on them represent the directions of information transmitted.

in which information is transmitted and processed, where V is the set of agents (nodes) with n agents and E is the set of edges. In this paper, it is assumed that communication devices together with a local controller processor form an agent. Moreover, an agent that connects a BESS is called *controllable* agent since the outputs of BESS can be regulated. While the agent which connects PCC node is regarded as *uncontrollable* agent because the power flowing through the PCC node can't be controlled directly. In addition, renewable DGs work at the maximum power point tracking model (MPPT), so there aren't agents for these DGs which in turn reduces the costs of communication network.

Assume that there are n agents and m controllable agents on the network G , respectively. A diagonal matrix $D = [d_{ii}]_{n \times n}$ is adopted to represent the outgoing degrees of each node, for instance, if agent i has two outgoing edges and one self-loop, then $d_{ii} = 3$. Further, a diagonal matrix $R = [r_{ij}]_{n \times n}$ is used to distinguish controllable agents and uncontrollable agents, in which if agent i is a controllable one, then $r_{ii} = 1$. Otherwise, $r_{ii} = 0$.

Moreover, as shown in Fig.1, each controllable agent connects a BESS through a directed dash line, where the direction of a arrow represents the direction of information transmission. On one hand, agents not only collect the present states of BESSs to which they connects, but also send instructions to BESSs. On the other hand, agents can transmit collected information to their neighbors on the communication network and process received information. Further, the power mismatch of whole MG system will be measured at the PCC node. Therefore, an uncontrollable agent, which connects the PCC node, is applied to collect the information of the system power mismatch. Under the configuration, the fluctuation of renewable energy sources will be smoothed by the microgrid

which prevents overloading in the PCC node and also leads to small impacts to grid.

B. DISTRIBUTED SOC BALANCING CONTROL LAWS

From the works [37] and [39], it is available to assume that the simplified calculation of SOC of a BESS can be written as,

$$soc_i(k) = soc_i(0) - z \cdot \int_0^k \hat{p}_i(k) dk \quad (1)$$

where $0 < z = \frac{1}{C_i \cdot V_i}$ is a constant, $\hat{p}_i(k)$ active outputs power of the controllable BESS $_i$. C_i and V_i are capacity, input voltage of converter, respectively. Therefore, the SOC of a BESS can be adjusted by regulating the discharging/charging power $\hat{p}_i(k)$. And $\hat{p}_i(k)$ is derivative of $soc_i(k)$, where the dynamics of a BESS can be simplified as a second-order system. Borrowing idea from the high-order consensus algorithm [40], a second-order distributed control law for MGs with renewable energy sources and BESSs was proposed. In order to guarantee the SOC of BESSs balanced, the following distributed control laws for controllable agents are provided according to the graph G ,

$$R \cdot P(k) = R \cdot \left(P(k-1) - \alpha \cdot F \cdot S(k-1) + F \cdot P(k-1) \right) \quad (2)$$

where $S(k-1) = [soc_i(k-1)]_{n \times 1}$, $P(k) = [p_i(k)]_{n \times 1}$, $P(k-1) = [p_i(k-1)]_{n \times 1}$ are column vectors of SOC and active power, while $\alpha > 0$ ($\alpha < 1/z$) is a constant that has influence on convergent property. And $F = [f_{ij}]_{n \times n}$ is the weighted matrix for the graph G , whose element is defined as

follows,

$$f_{ij} = \begin{cases} -\sum_{j=1, j \neq i}^m \delta, & j = i, \quad j \in N_i \cap L \\ \delta, & i \neq j, \quad j \in N_i \cap L \\ \frac{1}{d_g}, & j \in L' \\ 0, & \text{otherwise} \end{cases} \quad (3)$$

where $0 < \delta < \frac{1}{d_{max}}$ ($d_{max} = \max\{d_i | i = 1, \dots, n.\}$) is a constant, while N_i denotes a set of the neighbors of agent i . d_g is the outgoing degrees of the uncontrollable agent. L is a set of controllable agents, while L' denotes the complement of L , which is a set of uncontrollable agents.

Obviously, the proposed control laws (2) are totally distributed due to the fact that only the neighboring information soc_j and p_j are needed. Besides, it is proved that the SOC of BESSs converge and the system power is balanced through the iterative process if the controllable agents regulate the outputs of their BESSs in terms of control laws (2). In summary, for any given network, a distributed SOC balancing control law can be designed according to our proposed method, where only the attribute matrix R and the weighted matrix F of communication network G are needed. Moreover, control gain α , which helps to enhance the convergent speed, is added into the control law. One can design the distributed SOC balancing control laws with the knowledge of outgoing degrees of communication network. Compared with the algorithm in [29], the design of SOC balancing state variable and the local power supply-demand mismatch are avoided. The range of control gain for SOC is given via the simple way compared with the studies in [32], where the control algebraic Riccati equation needs to be solved to acquire feedback control gain with the demand of computation.

C. DISTRIBUTED REACTIVE POWER SHARING

In this subsection, we provide the distributed control laws for controllable agents, which are derived from the graph G , to ensure the reactive power shared reasonably among controllable BESS, i.e., proportional outputs of reactive power to their maximal reactive power. The distributed control laws for reactive power sharing are designed as follows,

$$R \cdot Q(k) = R \cdot H \cdot Q(k - 1), \quad (4)$$

where $H = [h_{ij}]_{m \times m}$ is a weighted matrix. And the entry of the matrix H is designed as follows,

$$h_{ij} = \begin{cases} 1 - \sum_{i=1, i \neq j}^n \frac{\theta}{q_i^{max}}, & j = i, \quad j \in N_i \cap L \\ \frac{\theta}{q_i^{max}}, & i \neq j, \quad j \in N_i \cap L \\ \frac{1}{d_g}, & j \in L' \\ 0, & \text{otherwise} \end{cases} \quad (5)$$

where $\theta \in (0, \frac{q_{min}^{max}}{d_{max}})$ is a constant, $Q^{max} = [q_i^{max}]_{n \times 1}$ reactive power capacity and $q_{min}^{max} = \min(q_i^{max} | i = 2, \dots, n)$, where $\theta \in (0, \frac{q_{min}^{max}}{d_{max}})$ is a constant, $Q^{max} = [q_i^{max}]_{n \times 1}$ reactive power capacity and $q_{min}^{max} = \min(q_i^{max} | i = 2, \dots, n)$.

Also, the proposed control laws (4) are fully distributed, since they only need the neighbors' information. Moreover, it can be proved that the distributed control laws (4) can both guarantee the proportional outputs and keep the reactive power balanced through iteration. Apparently, when the network of an MG is given, the distributed control laws for an MG will be designed in terms of the methods mentioned above. In addition, we will give explicit proofs for these proposed distributed control laws in section III.

Briefly, the process of building SOC balancing and reactive power sharing approach is,

Step 1: Build the communication network G , from which the outgoing degree matrix D and attribute matrix R are calculated.

Step 2: Calculate the weight matrix F and matrix H according to matrix R and D .

Step 3: Based on matrix F , build the second order control law (2) by adding the control gain ($\alpha < 1/z$). Based on H , build the control law (4).

Step 4: Each controllable agent collects the information of $\hat{p}_j(k - 1)$, $s\delta c_j(k - 1)$ and $\hat{q}_j(k - 1)$ from its neighbors, and then calculates the output ($\hat{p}_i(k)$, $\hat{q}_i(k)$) of BESS $_i$ at the step k according to equation (8) and (14).

Step 5: Send $\hat{p}_i(k)$, and $\hat{q}_i(k)$ to its BESS $_i$ and adjust the output of BESS $_i$.

III. CONVERGENCE ANALYSIS

In this section, we provide two theorems to analyze the convergence property for the proposed distributed control laws. The theorem 1 is introduced, which serves to ensure the system power demand-supply balanced and the SOC of BESSs converged when distributed control laws (2) are applied. Furthermore, the theorem 2 explains the convergence of the control laws (4).

Theorem 1: Supposing there is a directed communication network G with n agents over the MG, if the controllable agents adjust the active outputs power of BESSs in accordance with the control laws (2), these two conclusions are achieved,

1): The system power demand-supply is balanced, i.e., $\sum \hat{P}(k) = P_y(0)$;

2): The SOC of BESS $_{2, \dots, m}$ will converge, i.e., $soc_2(k) = soc_3(k) = \dots = soc_m(k) |_{k \rightarrow \infty}$.

Proof: 1) Assume y th agent is the uncontrollable agent, and if the both sides of equation (2) are summed up respectively, it yields,

$$\sum_{i=1}^n P(k)$$

$$\begin{aligned}
 &= \sum_{i=1}^n R \cdot P(k-1) - \sum_{i=1}^n \alpha \cdot R \cdot F \cdot S(k-1) \\
 &\quad + \sum_{i=1}^n F \cdot P(k-1) \\
 &= [r_{11}p_1(k-1) + \dots + r_{yy}p_y(k-1) \\
 &\quad + \dots + r_{ii}p_i(k-1) + \dots + r_{nn}p_n(k-1)] \\
 &\quad - \alpha \left[r_{11} \sum_{i=1}^n f_{1i}s_i(k-1) + \dots + r_{yy} \sum_{i=1}^n f_{yi}s_i(k-1) \right. \\
 &\quad \left. + \dots + r_{jj} \sum_{i=1}^n f_{ji}s_i(k-1) + \dots + r_{nn} \sum_{i=1}^n f_{ni}s_i(k-1) \right] \\
 &\quad + \sum_{i=1}^n f_{1i}p_1(k-1) + \dots + \sum_{i=1}^n f_{yi}p_i(k-1) \\
 &\quad + \dots + \sum_{i=1}^n f_{ji}p_i(k-1) + \dots + \sum_{i=1}^n f_{ni}p_i(k-1). \quad (6)
 \end{aligned}$$

Due to $f_{1i} + f_{2i} + \dots + f_{ii} + \dots + f_{ni} = 1$, the above equation can be reexpressed as follows:

$$\begin{aligned}
 \sum_{i=1}^n R \cdot P(k) &= [r_{11}p_1(k-1) + \dots + r_{yy}p_y(k-1) \\
 &\quad + \dots + r_{ii}p_i(k-1) + \dots + r_{nn}p_n(k-1)] \\
 &= \sum_{i=1}^n \hat{p}_i(k) = \sum_{i=1}^n \hat{p}_i(k-1) + p_y(k-1) \\
 &= \dots = p_y(0), \quad (7)
 \end{aligned}$$

where $\hat{p}_i(k-1)$ is the active set points of BESS_{*i*}, $p_y(k-1)$ is the system power mismatch at time step $k-1$ collected by the uncontrollable agent y . The equation (7) represents that the mismatch of system active power is shared by BESSs when control laws (2) is applied, which implicates the system active power is balanced.

2) Assume \tilde{F} is a weight matrix of controllable agents, the control laws (2) can be reduced to the following forms if the system power mismatch is shared by BESSs, i.e., when $p_y = 0$,

$$\hat{P}(k) = \hat{P}(k-1) - \alpha \cdot \tilde{F} \cdot \tilde{S}(k-1) + \tilde{F} \cdot \hat{P}(k-1), \quad (8)$$

where $\tilde{S}(k-1) = [\tilde{s}_i(k-1)]_{m \times m}$, $\hat{P}(k-1) = [\hat{p}_i(k-1)]_{m \times m}$ are the SOC column vectors, the active power column vectors of BESSs. Taking into account continuous form of (8), it yields,

$$\begin{bmatrix} \dot{S}(k) \\ \dot{\hat{P}}(k) \end{bmatrix} = Y \cdot \begin{bmatrix} \tilde{S}(k) \\ \hat{P}(k) \end{bmatrix}, \quad (9)$$

where

$$Y = \begin{bmatrix} 0_m & -\alpha \cdot I_m \\ -\alpha \cdot \tilde{F}_m & \tilde{F}_m \end{bmatrix}, \quad (10)$$

and the definition of matrix \tilde{F} is,

$$f_{ij} = \begin{cases} -\sum_{j=1, j \neq i}^m \delta, & j = i, \quad j \in N_i \cap L \\ \delta, & i \neq j, \quad j \in N_i \cap L \\ 0, & otherwise \end{cases} \quad (11)$$

Assume that ζ, λ are eigenvalues of \tilde{F} and Y , respectively. According to theorem 3.1 of [40], we know that zero is a simple eigenvalue of \tilde{F} ($\zeta_1 = 0$) and all other eigenvalues ($\zeta_n \leq \dots \leq \zeta_3 \leq \zeta_2 \leq 0$) have negative real parts. Moreover, it can be proved that following expression stands,

$$\lambda^2 - \zeta \cdot \lambda - \alpha \cdot z \cdot \zeta = 0. \quad (12)$$

Analyzing expression (12), we can find that, if $\zeta = 0$, matrix Y has two zero eigenvalues. If $\zeta \neq 0$, the root of the equation (12) is $\lambda = (\zeta \pm \sqrt{\zeta^2 + 4\alpha z \zeta})/2$, which implicates that matrix Y has two zero eigenvalues and all the other eigenvalues have negative real parts due to $\zeta \leq 0$. Thus, the convergence of proposed control laws (2) achieves gradually, i.e., $\tilde{s}_1(k) = \tilde{s}_2(k) = \dots = \tilde{s}_m(k)|_{k \rightarrow \infty}$, $\hat{p}_1(k) = \hat{p}_2(k) = \dots = \hat{p}_m(k)|_{k \rightarrow \infty}$. Moreover, the convergent speed of control laws (9) is associated to the parameter α and ζ , according to the theorem 1 in [41]. More specifically, the exponential decay is $\exp(-\sqrt{\alpha} \sqrt{z \zeta_2 \zeta_n} / (\zeta_2 - \zeta_n))$.

Theorem 2: On the graph G , if the controllable agents regulate the reactive power outputs of BESSs, the system reactive power demand-supply is still balanced. Besides, the proportional outputs of reactive power to their maximal reactive power will be reached, satisfying $\beta_1 = \beta_2 = \dots = \beta_m = \sum \hat{q}_i(0) / \sum q_i^{max}$.

Proof: If the both sides of equation (4) are summed up respectively, we have,

$$\begin{aligned}
 &\sum_{i=1}^n R \cdot Q(k) \\
 &= [r_{11}q_1(k) + \dots + r_{yy}q_y(k) \\
 &\quad + \dots + r_{ii}q_i(k) + \dots + r_{nn}q_n(k)] = \sum_{i=1}^n \hat{q}_i(k-1) \\
 &= \left[r_{11} \sum_{i=1}^n h_{1i}q_i(k-1) + \dots + r_{yy} \sum_{i=1}^n h_{yi}q_i(k-1) \right. \\
 &\quad \left. + \dots + q_{jj} \sum_{i=1}^n h_{ji}q_i(k-1) + \dots + r_{nn} \sum_{i=1}^n h_{ni}q_i(k-1) \right] \\
 &= (h_{11} + \dots + h_{i1} + \dots + h_{n1}) q_1(k-1) \\
 &\quad + \dots + (h_{1y} + \dots + h_{iy} + \dots + h_{ny}) q_y(k-1) \\
 &\quad + \dots + (h_{1n} + \dots + h_{in} + \dots + h_{nn}) q_n(k-1) \\
 &= q_1(k-1) + \dots + q_n(k-1) + q_y(k-1) \\
 &= \sum_{i=1}^n \hat{q}_i(k-1) + q_y(k-1), \quad (13)
 \end{aligned}$$

where $\hat{q}_i(k-1)$, $i = 1, \dots, m$ is the reactive outputs power of BESS_{*i*}. The equation (13) shows that the mismatch of system

reactive power is shared by BESSs when control laws (4) is applied, which maintains the system reactive power balanced.

Next, the convergence of the control laws (4) are analyzed as follows. Also, the control laws (4) will change into following forms, after the reactive power is shared among BESSs. Assume \tilde{H} is a weight matrix of controllable agents, we have,

$$\hat{Q}(k) = \tilde{H}\hat{Q}(k - 1), \quad (14)$$

where the entry of matrix \tilde{H} is defined as follows,

$$\tilde{h}_{ij} = \begin{cases} 1 - \sum_{i=1, i \neq j}^n \frac{\theta}{q_i^{max}}, & j = i, \quad j \in N_i \cap L \\ \frac{\theta}{q_i^{max}}, & i \neq j, \quad j \in N_i \cap L \\ 0, & otherwise \end{cases} \quad (15)$$

Multiplying the i th row of \tilde{H} by the column vector Q^{max} , it yields,

$$\begin{aligned} & h_{i1} \cdot q_1^{max} + \dots + h_{ii} \cdot q_i^{max} + \dots + h_{im} \cdot q_m^{max} \\ &= \frac{\theta}{q_1^{max}} \cdot q_1 + \frac{\theta}{q_2^{max}} \cdot q_2 + \dots + \frac{\theta}{q_m^{max}} \cdot q_m \\ &+ \dots + \left(1 - \frac{\theta}{q_i^{max}} - \dots - \frac{\theta}{q_i^{max}}\right) \cdot q_i^{max} = q_i^{max}, \end{aligned} \quad (16)$$

so $\tilde{H} \cdot Q^{max} = Q^{max}$.

If the topology of the communication network G is given, a conclusion that $\rho(\tilde{H}) \leq 1$ is arrived, where $\rho(\cdot)$ is the spectral radius of the matrix \tilde{H} . Let $U = \left(\tilde{H} - \frac{Q^{max} \cdot 1^T}{1^T \cdot Q^{max}}\right)$, then the expression $\rho(U) = \rho_2(\tilde{H}) < 1$ holds, where $\rho_2(\tilde{H})$ is the second largest eigenvalue of the matrix \tilde{H} . One can refer to our previous work [27] to obtain the explicit explains. Therefore, according to the conclusion of the document [42], we can obtain the following results,

$$\lim_{k \rightarrow \infty} (\tilde{H})^k = \frac{Q^{max} \cdot 1^T}{1^T \cdot Q^{max}}. \quad (17)$$

Thus, we have,

$$\begin{aligned} \lim_{k \rightarrow \infty} \hat{Q}(k) &= \lim_{k \rightarrow \infty} (\tilde{H})^k \cdot \hat{Q}(0) = \frac{Q^{max} \cdot 1^T}{1^T \cdot Q^{max}} \cdot \hat{Q}(0) \\ &= \left(\frac{\sum_{i=1}^m \hat{q}_i(0)}{\sum_{i=1}^m q_i^{max}}\right) \cdot Q^{max} \\ &= \beta \cdot Q^{max}. \end{aligned} \quad (18)$$

where $\hat{Q}(0)$ and β are the initial reactive outputs vector for DGs and the final proportion each BESSs reached, respectively.

IV. SYSTEM ARCHITECTURE

The simulation is conducted in MATLAB/Simulink environment to test the proposed control methods for Grid-connected microgrids shown in Fig. 1, which contains five uncontrollable DGs, five BESSs and ten loads. And the agent based communication network is also built on the MATLAB Function block in MATLAB/SIMULINK. Next, five uncontrollable DGs(DG_{7,8,9,10,11}) works at the maximum power

TABLE 1. Setup and parameters of BESSs, DGs and loads.

Sources	P^{max}, Q^{max}	Control	Load	Max.Demand
DG ₇	30 kW, 0 kVar	MPPT	Load ₇	40 kW, 30 kVar
DG ₈	50 kW, 0 kVar	MPPT	Load ₈	35 kW, 50 kVar
DG ₉	45 kW, 0 kVar	MPPT	Load ₉	35 kW, 45 kVar
DG ₁₀	55 kW, 0 kVar	MPPT	Load ₁₀	20 kW, 55 kVar
DG ₁₁	60 kW, 0 kVar	MPPT	Load ₁₁	25 kW, 60 kVar
BESS ₂	55 kW, 35 kVar	PQ	Load ₂	35 kW, 0 kVar
BESS ₃	45 kW, 25 kVar	PQ	Load ₃	50 kW, 0 kVar
BESS ₄	60 kW, 30 kVar	PQ	Load ₄	35 kW, 0 kVar
BESS ₅	70 kW, 45 kVar	PQ	Load ₅	35 kW, 0 kVar
BESS ₆	40 kW, 40 kVar	PQ	Load ₆	45 kW, 0 kVar

point tracking (MPPT) control mode, while the BESS_{2,3,4,5,6}, which belong to Lead-Acid battery, are working in the PQ control mode. Moreover, physical constraints are considered, when the simulation system of the MG is established. The outputs of uncontrollable DGs can't be greater than their maximal capacities or less than zero, while the outputs of a BESS can't be greater its maximal discharging power \hat{p}_i^{max} or less than maximal charging power $-\hat{p}_i^{min}$ ($\hat{p}_i^{min} = \hat{p}_i^{max}$). Further, it assumes that the uncontrollable DGs don't produce any reactive power, i.e., $Q_{7,8,9,10,11} = 0$ kVar. And the system voltage and the system frequency are set at 380V, 50Hz, respectively, while the line losses in the MG are considered, when the line impedance is set at $0.169 + j0.07\Omega/\text{km}$ [15]. In addition, the capacities of all BESSs are set at 20Ah [43], while the initial SOC states of BESS_{2,3,4,5,6} are set to {66%, 62%, 64%, 65%, 63%}. The rest of parameters are summarized in Table 1. Note that the system works in a balance state at the initial time.

Furthermore, *asynchronous communication* is adopted in this paper to reduce the information transmission and communication cost. Assume each agent has three $1 \times n$ vectors, $J^p(k) = [j_i^p(k)]_{1 \times n}$, $J^q(k) = [j_i^q(k)]_{1 \times n}$, $J^{soc}(k) = [j_i^{soc}(k)]_{1 \times n}$, to store the values of active and reactive power, the SOC of neighboring agent and its own. For example, if the absolute value of the difference $|j_i^{soc}(k) - soc_i(k)| \geq \Delta_1$, ($\Delta_1 > 0$), then the vector $J^{soc}(k)$ updates its entry $j_i^{soc}(k) = soc_i(k)$. After that, the agent send the value $soc_i(k)$ to its neighbors. Otherwise, the vector $J^{soc}(k)$ will not update its value and information transmission will not occur. Similarly, if the absolute difference $|j_i^p(k) - \hat{p}_i(k)| \geq \Delta_2$ (kW) ($\Delta_2 > 0$) or /and $|j_i^q(k) - \hat{q}_i(k)| \geq \Delta_3$ (kVar) ($\Delta_3 > 0$), the update of the vectors $J^p(k)$ or/and $J^q(k)$ will happen and the information transmission will occur. Once one of these vectors update theirs entries, agents will calculate the set points according to the control laws (2) and/or (4) to regulate the outputs of BESSs. For example, if the present information collected by agent _{i} $|j_i^p(k) - \hat{p}_i(k)| \geq \Delta_2$ (kW), agent _{i} will transmit the data $\hat{p}_i(k)$ to its neighbors and update the its vector $j_i^p(k) = \hat{p}_i(k)$. Moreover, agent _{i} will calculate the set-point of its connecting BESS in terms of the proposed control laws if agent _{i} updates its vector. Therefore, the parameters, Δ_1 , Δ_2 (kW) and Δ_3 (kVar), help to reduce the number of communications and release the burden of communication system. It is not difficult to understand that if the difference

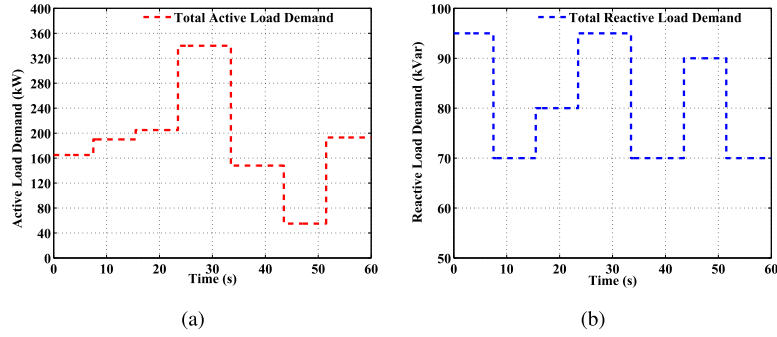


FIGURE 2. (a) Active power load-demand fluctuates over time. (b) Reactive power load-demand fluctuates over time.

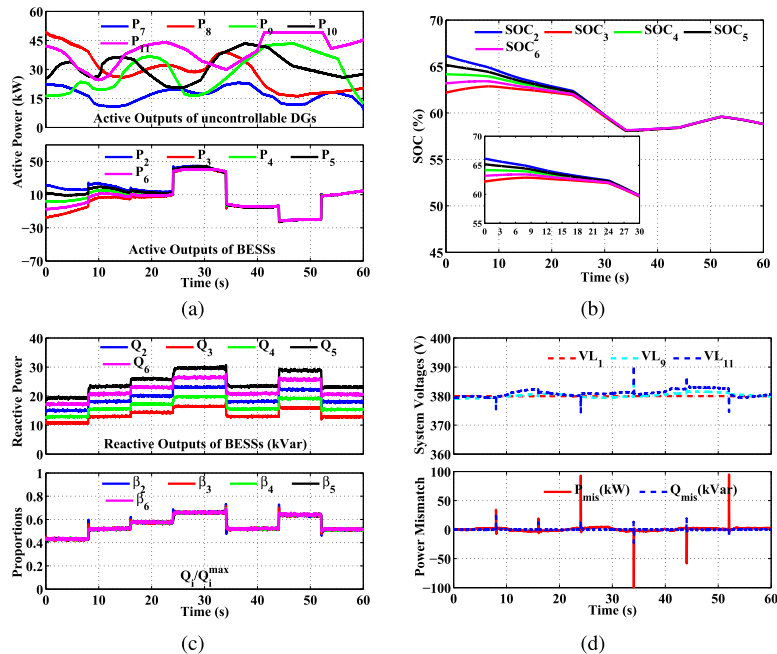


FIGURE 3. Simulation results on network G when both environmental conditions and load demand fluctuate. (a) is the active power outputs of uncontrollable DGs and BESSs. (b) shows the SOC of BESSs. (c) is the reactive outputs and proportions of BESSs. (d) is the system voltages and the system power mismatch.

of output of BESS between present time and previous time is small enough, we can regard the state of the output of BESS as unchanged. Hence, new set-points of BESS are unnecessary to calculate.

V. SIMULATION RESULTS

In this section, five simulation cases are designed to evaluate the performance of the proposed control method, when both load demand and active power outputs of renewable DGs change at the same time. In case 1, the system performance between the change of environmental conditions, load demand are studied. Next, the SOC convergence property under different α is investigated. Later, different Δ , packet losses, communication link failures and communication delays on the communication network G are considered in Case C. Next, comparison with benchmark algorithm

is studied. Furthermore, application to demand response is investigated. Finally, all results are discussed and explained in detail.

A. CASE 1: IMPACTS WHEN BOTH ENVIRONMENTAL CONDITIONS AND LOAD DEMAND FLUCTUATE

In the MG, DG_{7,11} and DG_{8,9,10} are PVs and WTs respectively, whose outputs rely on environmental conditions. Moreover, the fluctuation of load demand is also considered, as shown in Fig. 2, where the maximal fluctuation of active and reactive load demand is 192kW and 25kVar. In this case, the proposed control laws (2) and (4) are applied for agents on the network G where δ , α and θ are set to 0.45, $1e4$ and $1.2e4$, and the asynchronous parameters Δ_1 , Δ_2 , Δ_3 are set to 0.1%, 100(kW), 100(kVar), respectively.

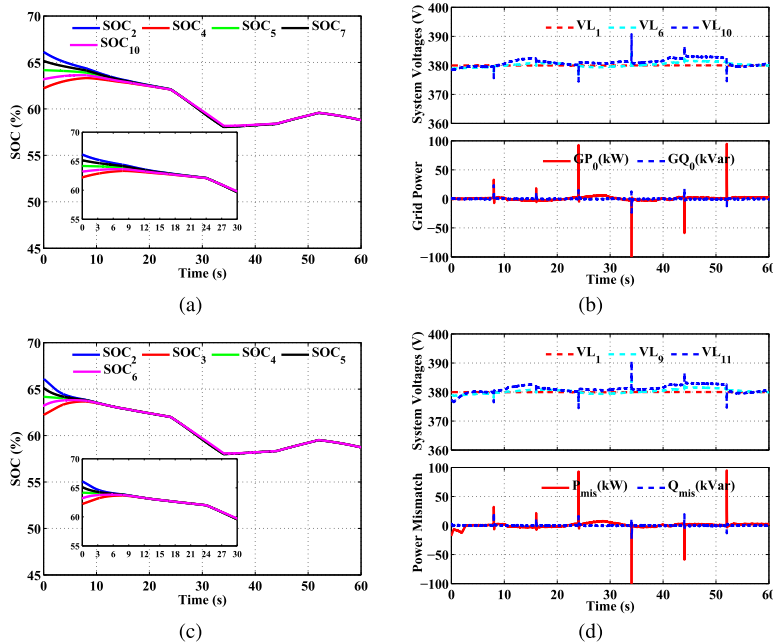


FIGURE 4. Simulation results with different α . (a) and (b) are obtained when α is $2e4$. (c) and (d) are obtained when α is $5e4$.

The results are shown in Fig. 3, where Fig. 3(a), (b) and (c) show the outputs of DGs and BESSs, the states of SOC, the system voltages at Load_{1,9,11} and power mismatch, respectively. From Fig.3(a), it can be found that the active power outputs of uncontrollable DGs change dramatically, while the active outputs power of BESSs become equal gradually due to the adjustment of provided control laws. Importantly, the SOC of BESSs converges slowly, which can be seen in Fig.3(b). Besides, reactive outputs power of BESSs are in proportion to their maximal reactive power, i.e., $\beta_2 = \beta_3 = \dots = \beta_6$, when both environmental conditions and load demand fluctuate drastically. Further, the system voltages vary slightly except the situations when load demand fluctuates severely. However, the voltages still stay close to 380V even in these situations. In addition, the system power mismatch always runs to zero, in addition to the moment when load demand fluctuates drastically, after BESSs are regulated by agents in terms of control laws (2) and (4).

In simulations, agents on the subgraph G send their information to their neighboring agents according to the asynchronous communication protocol. Later, controllable agents calculate the set points of BESSs according these information in terms of the control laws (2) and (4) in an iterative way. After calculation, controllable agents send these set points to local controllers to adjust the BESSs. However, the uncontrollable agent will not send messages to the PCC node since the power flowing though the PCC node can't be regulated directly. Eventually, the system active power and reactive power are dispatched as expectations, as shown in Fig. 3.

B. CASE 2: IMPACTS OF DIFFERENT PARAMETER α

From the control laws (2), it can be known that the parameter α has influence on the convergence of SOC of BESSs. Hence, in this subsection, the influence of different values of parameter α , i.e., $\alpha = 2e4, \alpha = 5e4$, to system performance are studied when control laws (2) are applied to controllable agents. And other settings are adopted as those in Case 1. The results are obtained in Fig.4.

Comparing the results in Fig.3(b) and Fig.4(a, c), it can be found that the convergent time of SOC, which are roughly 30s, 20s and 10s respectively, decreases as α becomes larger. However, the system voltages change in a normal range, still stay close to 380V, except the extreme conditions when load demand fluctuates drastically. At the beginning time, comparing Fig.4(b) and (d), the active power mismatch grows large when α increases, since the active power produced by BESSs and renewable DGs is larger than the sum of the load demand and maximal charging power of BESSs with lower SOC when considering output constraints of BESSs. Therefore, this part of active power is absorbed by the main grid.

C. CASE 3: IMPACTS OF DIFFERENT PARAMETER Δ , PACKET LOSSES, LINK FAILURES AND COMMUNICATION DELAYS

First, the impact of different parameter Δ is investigated. The asynchronous communication parameter Δ , which decides the amount of data transmitted on the communication network, has influence on the system performance. Here, we investigate the system performance under different $\Delta_2 = \Delta_3 = 300(\text{kW}, \text{kVar}), 500(\text{kW}, \text{kVar}) (\Delta_1 = 0.1\%)$ when the

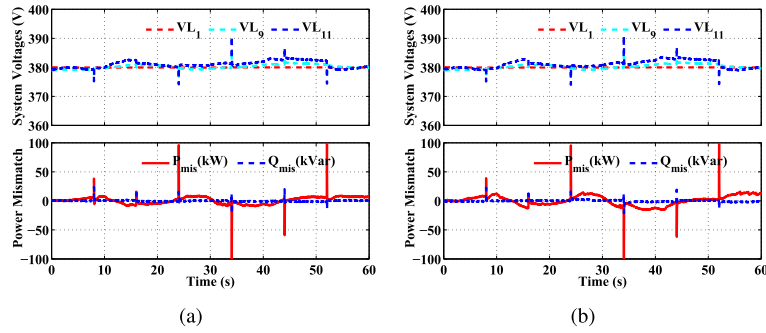


FIGURE 5. Simulation results with different Δ . (a) is obtained when Δ is 300. (c) is obtained when Δ is 500.

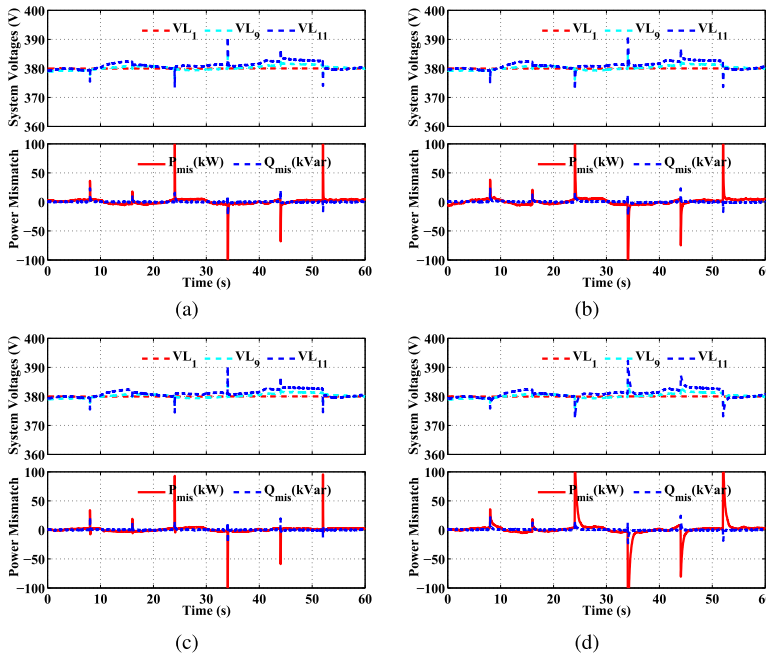


FIGURE 6. The system voltages and the system power mismatch with packet losses, link failures and communication delays. (a) and (b) are the system voltages and the system power mismatch when probability of packet losses is 0.3, 0.5. (c) is the system voltages with communication link failures. (d) is the system voltages with communication delays.

control laws (2) and (4) are applied by agents. Moreover, the other settings in this case follow those in Case 1. Simulation results are obtained as follows,

From Fig.5, one can see that the system runs well with different $\Delta_2 = \Delta_3 = 300(\text{kW}, \text{kVar}), 500(\text{kW}, \text{kVar})$, i.e., the SOC of BESSs and reactive power proportions converge gradually when environmental conditions and load demand fluctuate dramatically. Moreover, the system voltages still vary in an acceptable range. However, in comparison with Fig.3(d), the system power mismatch gets larger with the increasing of the Δ . When Δ becomes larger, the number of communication decreases, which means each agent will receive less information from its neighbors. And without latest information, BESSs will not share the system power mismatch well.

Second, the impact of packet losses in communication is studied. Information transmitted among agents may be lost

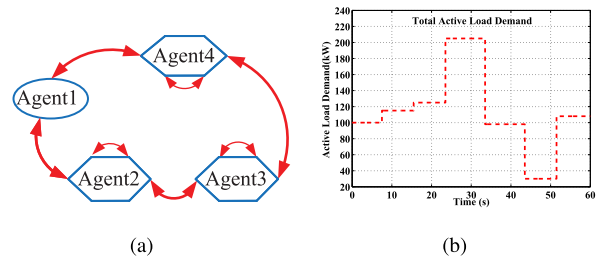


FIGURE 7. (a) is the communication network G_c for comparison. (b) is the active load demand.

when a communication network works unstable. Therefore, in this case, how packet losses on the graph G influence the system performance is investigated, when both environmental conditions and load demand fluctuate with the settings following those in Case 1. Assume that the probability of packet losses is set 0.3, 0.5 respectively, when information is

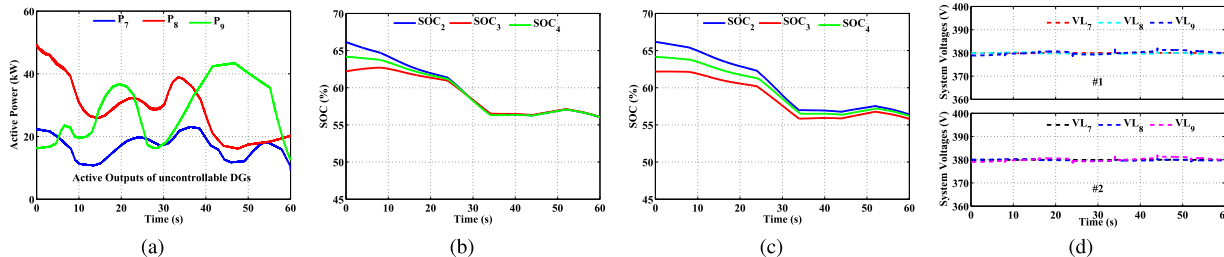


FIGURE 8. Simulation results with comparison. (a) is the active power outputs of uncontrollable DGs. (b) is the SOC of BESSs obtained from our methods. (c) is the SOC of BESSs obtained from methods in [32]. (d) is the system voltages obtained from both methods.

transmitted from agent_i to agent_j on the communication network. The statistical results in Fig. 6 (a) and (b) show that the system works stably, i.e., the system voltages are still close to 380V meanwhile the system power mismatch is almost zero. However, the system power mismatch in Fig. 6(a) is smaller than that in Fig. 6(b), due to the fact that the larger the probability of packet losses is the fewer the latest data processed successfully by agents. According to the results in Fig. 6, the small probability of packet losses less than 0.5 on communication network *G* will not deteriorate the system performance significantly.

As mentioned in Fig. 6(a, b), the system performance will not deteriorate significantly when packet losses occurring on the communication network. Hence, the impacts of an extreme condition, communication link failures, is investigated when system is running. Suppose that a communication link from agent₂ to agent₃ on the communication network *G* is broken at $k = 8s$ and then connected at $k = 24s$ with other settings follow those in case 1. Simulation results, as shown in Fig.6(c), indicate that the performance of the system isn't impacted negatively, i.e., the system is still stable and system voltages still close to 380V. The reason is that information of the system power mismatch is still collected and transmitted to controllable agents by uncontrollable agent₁, and at the same time each controllable agent still communicates with its neighboring controllable agents to reach a consensus on the SOC and proportions. However, it should be noted that there is at least one link from an uncontrollable agent to a controllable agent on the graph *G*, and the communication network composed by controllable agents should be connected.

Finally, the impacts of communication delays that may exist in a real-communication network are studied when both environmental conditions and load demand fluctuate, where other settings follow those in Case 1. Here, assume Gaussian random time delay $\tau_d \sim N(30ms, 20ms)$ happens on the communication network when information is transmitted among agents. Statistical results are obtained in Fig.6(d). As shown in Fig.6(d), the system still runs smoothly. However, compared with the results without time delays(Fig.3(d)), the system power mismatch takes a longer time to return zero, since agents at time t always calculate the set points of BESSs with the information received at time $t - \tau_d$. In this case, agents can't share the system power mismatch immediately.

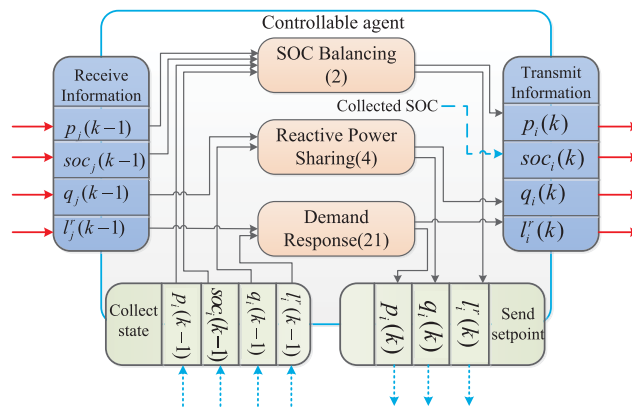


FIGURE 9. Agents with control laws.

D. CASE 4: COMPARISON WITH THE EXISTED ALGORITHM

As discussed in Section I, with the comparison of the previous works (see [22], [29], [30], [32]), this paper provides a systematic guideline to build distributed control model to achieve the balancing of SOC and system power as well as to keep system reactive power dispatched proportionally among BESSs, meanwhile, lifting some complicate restrictions on the design of control laws. Therefore, in order to give comparison, the control laws (14) of Section D in [32] with three BESSs are embedded into our model. The communication network *G_c* is shown in Fig. 7 [32] and the parameters $\alpha = 1e4$. The initial value of SOC is {66%, 62%, 64%} and the initial power of BESSs is 25, 33, 45(kW), respectively. Next, the parameters in control laws (14) are chosen as $cK_1 = -0.0822$, $cK_2 = 0.042$ [32]. Moreover, in order to test the system performance of the two methods, three BESSs, three renewable generations and six loads are built in our model. In simulation, active load demand is time-varying, ranging from 30 kW to 205 kW (Fig. 7(b)), while the outputs of uncontrollable DGs fluctuate from 8 kW to 50 kW. Simulation results show in Fig. 8. From the Fig. 8(b,c), it can be seen that SOC of BESSs in (b) (obtained from our method) converges faster than the SOC of BESSs in (c) (obtained from method in [32]), which shows improvements of our control laws. Besides, the system voltages are stable, staying close to 380V, since the system power is balanced during the iteration with both two methods.

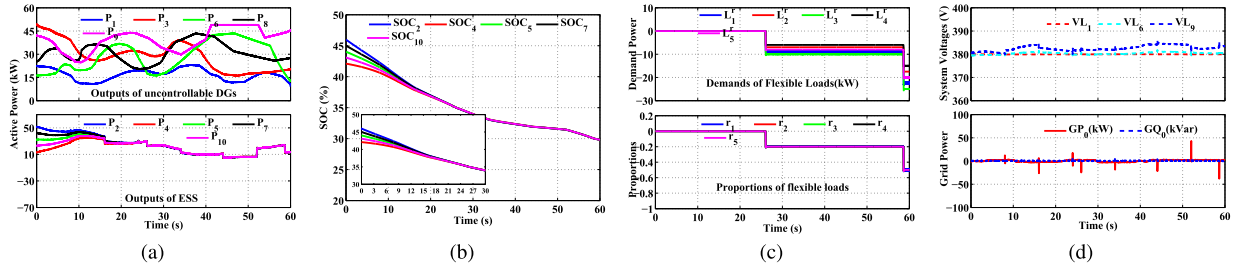


FIGURE 10. The performance of demand response. (a) is the active power outputs of uncontrollable DGs. (b) is the SOC of BESSs. (c) is the adjusted power of flexible loads. (d) is the system voltages and system power mismatch.

TABLE 2. Parameters of flexible loads.

Flexible Loads	$L_i^{rmax}(kW)$	$L_i^{rmin}(kW)$
L_1^r	50 kW	5 kW
L_2^r	45 kW	10 kW
L_3^r	55 kW	5 kW
L_4^r	35 kW	5 kW
L_5^r	40 kW	0 kW

E. CASE 5: APPLICATION TO DEMAND RESPONSE

The SOC balancing, reactive power sharing and demand response can be achieved concurrently by our approach if agents adjust the BESS and flexible loads in terms of control laws (2), (4) and (21). As it can be seen in Fig. 9, three different control laws are embedded into the controllable agents, where expressions (2), (4) and (21) are the SOC balancing, reactive power sharing and demand response control laws, respectively. With the received information and collected states, controllable agents will finish the task of SOC balancing, reactive power sharing and demand response in a distributed way. In order to validate the effectiveness of proposed method, the demand response is investigated. Here, we assume that five loads, Load₆, Load₇, Load₈, Load₉ and Load₁₀ in microgrid, are flexible loads, which means that these loads are adjustable. In order to extend proposed methods to this area, we assume that controllable agents also collect the states of flexible loads, that is, bidirected communication lines are added between flexible loads and controllable agent₆, agent₂, agent₃, agent₄ and agent₅. Their parameters are shown in Table 2. Besides, controllable agents also collect information from flexible loads, after computation, send setpoints to flexible loads. Thereafter, the flexible load adjusts its demand according to the setpoints. In addition to collecting the system power loss, uncontrollable agent will also provide strategy to start the process of demand response with the information of market condition, renewable generation and SOC of BESS.

Here, we use the SOC as the variable to achieve the coordination between BESSs and flexible loads. Assume that the process of demand response is started as the SOC of BESSs reaches threshold value. Uncontrollable agent calculate the amount of adjustable power ΔL_p according to the formula (19),

$$\Delta L_p(k) = r(k) \left(\frac{\Delta L_i^r + \Delta L_j^r}{d_g} \right), \quad (19)$$

where $r(k)$ is proportion of adjustable power to maximal adjustable power of flexible loads, which is related with SOC of BESSs and the sum of maximal adjustable capacities of flexible loads,

$$r(k) = \begin{cases} -1, & 0.20 < soc(k) \leq 0.25 \\ -2.5, & 0.25 < soc(k) \leq 0.30 \\ -4, & 0.30 < soc(k) \leq 0.35 \\ 0, & 0.35 < soc(k) \leq 0.75 \\ 1, & 0.75 < soc(k) \leq 0.80 \\ 2.5, & 0.80 < soc(k) \leq 0.85 \\ 4, & 0.85 < soc(k) \leq 0.90. \end{cases} \quad (20)$$

$\Delta L_p(k)$ is the information of uncontrollable agent. Specially, if the SOC of BESSs is higher than 90% or lower than 20%, BESSs will stop charging or discharging and flexible loads will be the maximal or minimal demands. According to the (19), uncontrollable agent calculates the value of adjustable power $\Delta L_p(k)$ according to the received value of SOC from neighbors. Therefore, considering the network G , control laws for flexible loads are given as,

$$R(L^r(k)) = RH'(L^r(k-1)), \quad (21)$$

where $L^r(k) = [L_i^r(k)]_{m \times m}$ is the column of the adjustable power of flexible loads. If we replace q_i^{max} of control laws (4) with ΔL_i^r , the weighted matrix H is changed into H' . $\Delta L^r = [\Delta L_i^r]_{m \times m}$ is the column of the maximal adjustable power of flexible loads. Agents will regulate the adjustable power of flexible loads according to their maximal adjustable power in terms of the control laws (21). In other word, flexible loads will be adjusted according to their maximal adjustable power if the SOC of the BESSs reaches threshold value. It's worth mentioning that in order to adjust the potential flexible loads, we assume that the flexible loads are adjusted after control laws (21) converge. And that explains $|r(k)| > 1$. In this simulation, reactive power sharing is not considered.

Fig. 10 shows the results of demand response when flexible loads are considered. From the results shown in Fig.10(a) and (b), the active outputs and SOC of BESSs still converge even when load demand and environmental conditions change. Specially, the flexible loads adjust their load demand when SOC reaches 35% according to their maximal adjustable power. As it can be seen in Fig.10(c), the amount of adjusted

power is proportional to their maximal adjustable power. The proportions of flexible loads reach 0.2 at time(28s) when SOC is under 35%, and proportions are 0.5 at time(58s) when SOC is lower than 30%. Moreover, the system voltages still vary in a normal range, seen in Fig.10(d).

VI. CONCLUSION

This paper proposed a two layer distributed control method for grid-connected microgrids to manage the BESSs when the intermittent outputs of renewable DGs and the fluctuation of load demand are considered. The bottom layer is a grid-connected MG composed WTs, PVs, BESSs and Loads, while the top layer is a communication network which is consisted of agents. And agents adjust the outputs of BESSs according to the setpoints calculated by proposed distributed control laws. Correspondingly, a set of distributed control laws for agents are proposed from any given communication network, where the fast second-order control laws and the optimal control laws are designed for SOC balancing and reactive power sharing of BESSs, respectively. In addition, two theorems are introduced to analyze the property of the system power balance, the SOC balancing and proportional outputs of maximal reactive power among BESSs.

In order to test the performance of the control laws, five simulation cases are designed in MATLAB/SIMULINK, when both environmental conditions and load demand fluctuate dramatically. Simulation results show that the proposed control method can guarantee that the system works well, i.e., the system voltages vary in a normal range, while the SOC balancing and proportional outputs of BESSs are achieved, even if there are packet losses, communication delays, link failures occurring on the communication network during the simulation. Moreover, with the comparison of the existed methods, our approach offers a simple way to design the control laws from given communication network and has the fast convergent speed of SOC balancing. Besides, the proposed control method has the potential to the application of demand response. Furthermore, distributed optimization model for BESSs, which includes states of battery health, battery lifetime costs as well as charging/discharging current, in active distribution network is an interesting topic.

REFERENCES

- [1] D. Abbott, "Keeping the energy debate clean: How do we supply the world's energy needs?" *Proc. IEEE*, vol. 98, no. 1, pp. 42–66, Jan. 2010.
- [2] R. H. Lasseter, "Smart distribution: Coupled microgrids," *Proc. IEEE*, vol. 99, no. 6, pp. 1074–1082, Jun. 2011.
- [3] Q. Jiang and H. Wang, "Two-time-scale coordination control for a battery energy storage system to mitigate wind power fluctuations," *IEEE Trans. Energy Convers.*, vol. 28, no. 1, pp. 52–61, Mar. 2013.
- [4] R. Sebastián, "Application of a battery energy storage for frequency regulation and peak shaving in a wind diesel power system," *IET Gener., Transmiss. Distrib.*, vol. 10, no. 3, pp. 764–770, 2016.
- [5] T. Morstyn, B. Hredzak, and V. G. Agelidis, "Control strategies for microgrids with distributed energy storage systems: An overview," *IEEE Trans. Smart Grid*, vol. 9, no. 4, pp. 3652–3666, Jul. 2018.
- [6] C. Liu, X. Wang, X. Wu, and J. Guo, "Economic scheduling model of microgrid considering the lifetime of batteries," *IET Gener., Transmiss. Distrib.*, vol. 11, no. 3, pp. 759–767, 2017.
- [7] O. Palizban and K. Kauhaniemi, "Distributed cooperative control of battery energy storage system in AC microgrid applications," *J. Energy Storage*, vol. 3, pp. 43–51, Sep. 2015. [Online]. Available: <http://www.sciencedirect.com/science/article/pii/S2352152X15300074>
- [8] E. Perez, H. Beltran, N. Aparicio, and P. Rodriguez, "Predictive power control for PV plants with energy storage," *IEEE Trans. Sustain. Energy*, vol. 4, no. 2, pp. 482–490, Apr. 2013.
- [9] Y. Riffonneau, S. Bacha, F. Barruel, and S. Ploix, "Optimal power flow management for grid connected PV systems with batteries," *IEEE Trans. Sustain. Energy*, vol. 2, no. 3, pp. 309–320, Jul. 2011.
- [10] J. Cai, C. Chen, S. Duan, and D. Yang, "Centralized control of large capacity parallel connected power conditioning system for battery energy storage system in microgrid," in *Proc. IEEE Energy Convers. Congr. Expo. (ECCE)*, Sep. 2014, pp. 409–413.
- [11] G. Wang, M. Ciobotaru, and V. G. Agelidis, "Power smoothing of large solar PV plant using hybrid energy storage," *IEEE Trans. Sustain. Energy*, vol. 5, no. 3, pp. 834–842, Jul. 2014.
- [12] B. Hredzak, V. G. Agelidis, and M. Jang, "A model predictive control system for a hybrid battery-ultracapacitor power source," *IEEE Trans. Power Electron.*, vol. 29, no. 3, pp. 1469–1479, Mar. 2014.
- [13] N. L. Díaz, A. C. Luna, J. C. Vasquez, and J. M. Guerrero, "Centralized control architecture for coordination of distributed renewable generation and energy storage in islanded AC microgrids," *IEEE Trans. Power Electron.*, vol. 32, no. 7, pp. 5202–5213, Jul. 2017.
- [14] A. Bidram and A. Davoudi, "Hierarchical structure of microgrids control system," *IEEE Trans. Smart Grid*, vol. 3, no. 4, pp. 1963–1976, Dec. 2012.
- [15] Q. Li, F. Chen, M. Chen, J. M. Guerrero, and D. Abbott, "Agent-based decentralized control method for islanded microgrids," *IEEE Trans. Smart Grid*, vol. 7, no. 2, pp. 637–649, Mar. 2016.
- [16] Q. Li, C. Peng, M. Wang, M. Chen, J. M. Guerrero, and D. Abbott, "Distributed secondary control and management of islanded microgrids via dynamic weights," *IEEE Trans. Smart Grid*, vol. 10, no. 2, pp. 2196–2207, Mar. 2019.
- [17] M. A. Mahmud, M. J. Hossain, H. R. Pota, and A. M. T. Oo, "Robust nonlinear distributed controller design for active and reactive power sharing in islanded microgrids," *IEEE Trans. Energy Convers.*, vol. 29, no. 4, pp. 893–903, Dec. 2014.
- [18] A. Urtasun, E. L. Barrios, P. Sanchis, and L. Marroyo, "Frequency-based energy-management strategy for stand-alone systems with distributed battery storage," *IEEE Trans. Power Electron.*, vol. 30, no. 9, pp. 4794–4808, Sep. 2015.
- [19] H. Mahmood and J. Jiang, "Autonomous coordination of multiple pv/battery hybrid units in islanded microgrids," *IEEE Trans. Smart Grid*, vol. 9, no. 6, pp. 6359–6368, Nov. 2018. doi: [10.1109/TSG.2017.2709550](https://doi.org/10.1109/TSG.2017.2709550).
- [20] T. Morstyn, M. Momayyezani, B. Hredzak, and V. G. Agelidis, "Distributed control for state-of-charge balancing between the modules of a reconfigurable battery energy storage system," *IEEE Trans. Power Electron.*, vol. 31, no. 11, pp. 7986–7995, Nov. 2016.
- [21] M. S. Golsorkhi, Q. Shafiee, D. D.-C. Lu, and J. M. Guerrero, "A distributed control framework for integrated photovoltaic-battery-based islanded microgrids," *IEEE Trans. Smart Grid*, vol. 8, no. 6, pp. 2837–2848, Nov. 2017.
- [22] H. Cai and G. Hu, "Distributed control scheme for package-level state-of-charge balancing of grid-connected battery energy storage system," *IEEE Trans. Ind. Informat.*, vol. 12, no. 5, pp. 1919–1929, Oct. 2016.
- [23] H. S. V. S. K. Nouna and S. Doolla, "Multiagent-based distributed-energy-resource management for intelligent microgrids," *IEEE Trans. Ind. Electron.*, vol. 60, no. 4, pp. 1678–1687, Apr. 2013.
- [24] F. Chen, M. Chen, Q. Li, K. Meng, J. M. Guerrero, and D. Abbott, "Multiagent-based reactive power sharing and control model for islanded microgrids," *IEEE Trans. Sustain. Energy*, vol. 7, no. 3, pp. 1232–1244, Jul. 2016.
- [25] W. Liu, W. Gu, W. Sheng, X. Meng, Z. Wu, and W. Chen, "Decentralized multi-agent system-based cooperative frequency control for autonomous microgrids with communication constraints," *IEEE Trans. Sustain. Energy*, vol. 5, no. 2, pp. 446–456, Apr. 2014.
- [26] A. Bidram, A. Davoudi, F. L. Lewis, and J. M. Guerrero, "Distributed cooperative secondary control of microgrids using feedback linearization," *IEEE Trans. Power Syst.*, vol. 28, no. 3, pp. 3462–3470, Aug. 2013.
- [27] W. Kang et al., "Distributed secondary control method for islanded microgrids with communication constraints," *IEEE Access*, vol. 6, pp. 5812–5821, 2017.
- [28] D. H. Nguyen and J. Khazaei, "Multiagent time-delayed fast consensus design for distributed battery energy storage systems," *IEEE Trans. Sustain. Energy*, vol. 9, no. 3, pp. 1397–1406, Jul. 2018.

- [29] Y. Xu, Z. Li, J. Zhao, and J. Zhang, "Distributed robust control strategy of grid-connected inverters for energy storage systems' state-of-charge balancing," *IEEE Trans. Smart Grid*, vol. 9, no. 6, pp. 5907–5917, Nov. 2018.
- [30] C. Huang, S. Weng, D. Yue, S. Deng, J. Xie, and H. Ge, "Distributed cooperative control of energy storage units in microgrid based on multi-agent consensus method," *Electr. Power Syst. Res.*, vol. 147, pp. 213–223, Jun. 2017. [Online]. Available: <http://www.sciencedirect.com/science/article/pii/S037877961730086X>
- [31] X. Chang et al., "State-of-charge balancing control strategy based on discrete consensus algorithm for battery energy storage in islanded microgrid," in *Proc. 2nd IEEE Conf. Energy Internet Energy Syst. Integr. (EI2)*, Oct. 2018, pp. 1–6.
- [32] J. Khazaei and Z. Miao, "Consensus control for energy storage systems," *IEEE Trans. Smart Grid*, vol. 9, no. 4, pp. 3009–3017, Jul. 2018.
- [33] C. P. Nguyen and A. J. Flueck, "Agent based restoration with distributed energy storage support in smart grids," *IEEE Trans. Smart Grid*, vol. 3, no. 2, pp. 1029–1038, Jun. 2012.
- [34] Y. Xu, W. Zhang, G. Hug, S. Kar, and Z. Li, "Cooperative control of distributed energy storage systems in a microgrid," *IEEE Trans. Smart Grid*, vol. 6, no. 1, pp. 238–248, Jan. 2015.
- [35] Z. Li, C. Zang, P. Zeng, H. Yu, and S. Li, "Agent-based distributed and economic automatic generation control for droop-controlled AC microgrids," *IET Gener., Transmiss. Distrib.*, vol. 10, no. 14, pp. 3622–3630, 2016.
- [36] T. Morstyn, B. Hredzak, and V. G. Agelidis, "Distributed cooperative control of microgrid storage," *IEEE Trans. Power Syst.*, vol. 30, no. 5, pp. 2780–2789, Sep. 2015.
- [37] C. Li, E. A. A. Coelho, T. Dragicevic, J. M. Guerrero, and J. C. Vasquez, "Multiagent-based distributed state of charge balancing control for distributed energy storage units in AC microgrids," *IEEE Trans. Ind. Appl.*, vol. 53, no. 3, pp. 2369–2381, May/Jun. 2017.
- [38] Q. Li et al., "Networked and distributed control method with optimal power dispatch for islanded microgrids," *IEEE Trans. Ind. Electron.*, vol. 64, no. 1, pp. 493–504, Jan. 2017.
- [39] Y.-S. Kim, E.-S. Kim, and S.-I. Moon, "Frequency and voltage control strategy of standalone microgrids with high penetration of intermittent renewable generation systems," *IEEE Trans. Power Syst.*, vol. 31, no. 1, pp. 718–728, Jan. 2016.
- [40] W. Ren, K. Moore, and Y. Chen, "High-order consensus algorithms in cooperative vehicle systems," in *Proc. IEEE Int. Conf. Netw., Sens. Control*, Apr. 2006, pp. 457–462.
- [41] J. Zhu, "On consensus speed of multi-agent systems with double-integrator dynamics," *Linear Algebra Appl.*, vol. 434, no. 1, pp. 294–306, 2011. [Online]. Available: <http://www.sciencedirect.com/science/article/pii/S0024379510004325>
- [42] J. Liu and A. S. Morse, "Accelerated linear iterations for distributed averaging," *Annu. Rev. Control*, vol. 35, no. 2, pp. 160–165, 2011.
- [43] B. Zhao, X. Zhang, J. Chen, C. Wang, and L. Guo, "Operation optimization of standalone microgrids considering lifetime characteristics of battery energy storage system," *IEEE Trans. Sustain. Energy*, vol. 4, no. 4, pp. 934–943, Oct. 2013.



WENFA KANG received the B.S. degree in electrical engineering from the Chengdu University of Information Technology, Chengdu, China, in 2014, and the M.S. degree from the School of Electrical Engineering, Chongqing University, Chongqing, in 2017, where he is currently pursuing the Ph.D. degree. His current research interests include networked control systems, optimization of microgrids, battery energy storage systems, and active distribution networks.



MINYOU CHEN received the M.Sc. degree from Chongqing University, China, in 1987, and the Ph.D. degree in control engineering from The University of Sheffield, Sheffield, U.K., in 1998. He is currently a Full Professor with Chongqing University. He has authored or coauthored over 180 papers. His research interests include intelligent modeling and control, multiobjective optimization, micro-grid control, and state monitoring in power distribution systems.



BO LI received the B.E. degree in agricultural electrification and automation from Guangxi University, Nanning, China, in 2016. He is currently pursuing the Ph.D. degree in electrical engineering with Chongqing University, Chongqing, China. His current research interests include distributed optimization in multi-agent systems and distributed control in smart grid.



FEIXIONG CHEN (S'16–M'18) received the B.S. degree in electrical engineering from the Chongqing University of Technology, in 2012, and the Ph.D. degree in electrical engineering from Chongqing University, Chongqing, China, in 2017. From 2016 to 2017, he was a Visiting Ph.D. Student with the Department of Electrical and Computer Engineering, Wayne State University, Detroit, MI, USA. Since 2017, he has been a Research Associate with the Department of Electrical Engineering, The Hong Kong Polytechnic University, Hong Kong. He is currently a Lecturer with the School of Electrical Engineering and Automation, Fuzhou University, Fuzhou, China. His current research interests include distributed control and optimization of microgrids.



WEI LAI (M'18) received the M.Sc. degree from the Chongqing University of Technology, Chongqing, China, in 2012, and the joint Ph.D. degree from the University of Warwick, Coventry, U.K., in 2015, funded by the China Scholarship Council. He is currently a Lecturer in electrical engineering with the School of Electrical Engineering, Chongqing University, Chongqing. His current research interests include the reliability of power modules, the application of power electronics for electric power generation, and the development of condition monitoring methods for power electronic converters. He is also studying the application of power electronics for microgrids and energy storage systems.



HOUFEI LIN born in 1969. He received the bachelor's degree in electrical engineering and automation engineering from the Zhejiang Institute of Technology (Zhejiang University of Technology), in 1993. He is currently the Deputy General Manager and a Senior Engineer with Zhejiang Pingyang Power Supply Company of State Grid.



BO ZHAO received the Ph.D. degree from the Department of Electrical Engineering, Zhejiang University, Hangzhou, Zhejiang, China, in 2005. He is currently an Engineer with the State Grid Zhejiang Electric Power Research Institute, Hangzhou. His research interests include distributed generation and microgrids.

...